JOURNAL OF SOLID STATE CHEMISTRY 84, 289–298 (1990)

The Synthesis and Crystal Structures of the Related Series of Aluminoborates: $Co_{2.1}Al_{0.9}BO_5$, Ni_2AlBO_5, and Cu_2AlBO_5

J. A. HRILJAC, R. D. BROWN, AND A. K. CHEETHAM

University of Oxford, Chemical Crystallography Laboratory, 9 Parks Road, Oxford OX1 3PD, United Kingdom

AND L. C. SATEK

Amoco Chemical Company, P.O. Box 400, Naperville, Illinois 60566

Received August 21, 1989

We report on the growth of single crystals of Ni_2AlBO_5, Cu_2AlBO_5, and the mixed-valent $Co_{2.1}Al_{0.9}BO_5$ from borax fluxes. All of these materials have been studied by single-crystal X-ray diffraction. The nickel and cobalt compounds are isostructural with the natural mineral ludwigite, while the copper compound is a monoclinically distorted variant of this structure. All three compounds show nonrandom disorder of the transition metal and aluminium atoms over four crystallographically distinct metal sites. We discuss the structural effects of this disorder and attempt to rationalize the observed occupancies on the basis of covalent and ionic forces. Ni_2AlBO_5: orthorhombic, a = 12.013(1) Å, b = 9.111(1) Å, c = 2.942(1) Å, space group *Pbam*, Z = 4, R = 4.07%. $Co_{2.1}Al_{0.9}BO_5$: orthorhombic, a = 12.010(2) Å, b = 9.197(2) Å, c = 2.993(1) Å, space group *Pbam*, Z = 4, R = 4.44%. Cu_2AlBO_5: monoclinic, a = 9.365(1) Å, b = 11.778(2) Å, c = 3.072(2) Å, β = 97.71(2)°, space group $P2_1/a$, Z = 4, R = 4.59%.

Introduction

The diversity of borate anions, both in solution and solid state, makes borate chemistry as extensive as the more commonly studied areas of silicates and phosphates. Recent work in the area has demonstrated that the solid state borates display a wide range of interesting physical properties. Among the applications of borates are the use of compounds in the CuO–Al_2O_3–B_2O_3 system as selective mild dehydrogenation (*1*) and dehydrocyclization catalysts (*2*), and the exploitation of lanthanum aluminium borates (*3*) and β-$Ba_2B_2O_5$ (*4*) for their nonlinear optical properties.

For first row transition metal borates, one of the more common polytypes is the ludwigite structure, based on the natural mineral of approximate formula Mg_2FeBO_5 (*5*). This structure type, and its derivatives, are known for a wide variety of di-, tri-, and tetravalent metal ions (*6–11*). An early report of Ni_2AlBO_5 indicated this material was isostructural with ludwigite, but the poor agreement factor, from the analysis of the single-crystal X-ray diffraction data, indicated that the model was not completely correct (*7*). The copper analog of this material is listed in the Powder Diffraction File (*12*) but, to our knowledge, no structural investigation has been reported. The re-

0022-4596/90 $3.00

lated phase $Cu_9Al_3B_4O_{19.5}$ has been studied (*9*).

In this paper we report on the growth of single crystals of Ni_2AlBO_5, Cu_2AlBO_5, and the mixed-valent $Co_{2.1}Al_{0.9}BO_5$ from borax fluxes, and the results of subsequent X-ray diffraction experiments. We find the structures are related and report on the interesting distributions of the aluminum and transition metal ions over the various sites.

Experimental

Ni_2AlBO_5 was synthesized by grinding together NiO (0.158 g, 2.12 mmol) and $Na_2B_4O_7 \cdot 10H_2O$ (4.84 g, 12.70 mmol) and then packing the mixture into an alumina boat. The boat was placed in the center of a tube furnace and slowly heated to 1000°C, left at temperature for 10 hr, and then cooled at 20°C per hour. Pale green rod-like crystals were isolated after the melt was dissolved in dilute hydrochloric acid. Irregular-shaped green crystals of Cu_2AlBO_5 were synthesized in a similar fashion from CuO (0.325 g, 4.09 mmol) and $Na_2B_4O_7 \cdot 10H_2O$ (4.675 g, 12.26 mmol). A greater MO : borax ratio was used because CuO is more soluble in the melt. A second phase consisting of light-blue needles was formed as a minor product and its characterization will be reported elsewhere (*13*). Jet black needles of $Co_{2.1}Al_{0.9}BO_5$ were synthesized from Co_3O_4 (0.6 g, 2.5 mmol), Al_2O_5 (0.19 g, 1.9 mmol), and $Na_2B_4O_7 \cdot 10H_2O$ (2.0 g, 5.2 mmol), with a reaction time of 25 hr at 1000°C.

Analytical electron microscopy was performed with a JEOL 2000FX instrument, and element ratios were determined from the intensities of the characteristic X-ray emission peaks (*14*). The appropriate spinel materials were used as calibration standards.

A crystal of Ni_2AlBO_5 was glued onto the end of a glass fiber placed on an Enraf-Nonius CAD4-F diffractometer. Automatic search, indexing, and centering routines were used to obtain the unit cell and orientation matrix. The final cell was obtained by centering 24 high-angle reflections. The data were collected using the scan parameters shown in Table I. The intensities of three standard reflections were monitored every hour and indicated no crystal decay. Data for the other compounds were measured in a similar fashion.

For Ni_2AlBO_5, the systematic absences were consistent with the space groups *Pbam* and $Pba2_1$. *Pbam* was chosen and confirmed by the results of the refinement. The data were corrected for Lorentz and polarization effects, and an empirical absorption correction applied (*15*). The solution of Schwab and Bertaut was used as a starting model for the least-squares refinement (*7*). The occupancies of the metal sites were included in the refinement, with the overall stoichiometry constrained to give a Ni : Al ratio of 2 : 1 and with all of the metal sites fully occupied. The refinement converged, using unit weights, with an *R*-value of 4.46%. Application of a modified three-term Chebyschev polynomial weighting scheme (*16*) (which downweighted the 211, 002, and 162 reflections) followed by final refinement of positional parameters, anisotropic temperature factors, constrained metal site occupancies, and an extinction parameter converged to give a final *R*-factor of 4.07%. The results are summarized in Table I, with final fractional atomic coordinates, occupation numbers, and anisotropic temperature factors presented in Table II, and selected distances and angles listed in Table V. The computer programs RC85 (*17*) and CRYSTALS (*18*) were used throughout. Neutral atom-scattering factors were taken from Ref. (*19*). Structural diagrams were drawn with CHEM-X (*20*).

The data collection and reduction for $Co_{2.1}Al_{0.9}BO_5$ were treated in a similar fashion. During the refinement the metal sites were constrained to full occupancy, but no

TABLE I

DATA COLLECTION AND REFINEMENT PARAMETERS

Empirical formula	Ni_2AlBO_5	$Co_{2.1}Al_{0.9}BO_5$	Cu_2AlBO_5
Formula weight	235.17	238.85	244.88
Crystal size (mm)	0.03 × 0.05 × 0.80	0.02 × 0.02 × 0.18	0.05 × 0.05 × 0.40
Crystal system	Orthorhombic	Orthorhombic	Monoclinic
Space group	*Pbam*	*Pbam*	$P2_1/a$
a (Å)	12.013(1)	12.010(2)	9.365(1)
b (Å)	9.111(1)	9.197(2)	11.778(2)
c (Å)	2.942(1)	2.993(1)	3.072(2)
β (°)	90	90	97.71(2)
V (Å^3)	322.0	330.6	335.8
Z	4	4	4
D_c (g cm^{-3})	4.851	4.799	4.844
$F(000)$	456	448	464
X-radiation	Cu$K\alpha$	Mo$K\alpha$	Mo$K\alpha$
λ (Å)	1.5418	0.71069	0.71069
Linear abs. coefficient (cm^{-1})	164.8	106.4	128.6
θ range (°)	1–75	1–30	1–30
ω-scan width (°)	0.9 + 0.15 tan θ	0.8 + 0.35 tan θ	0.9 + 0.35 tan θ
Scan speed range (° min^{-1})	0.8–6.7	0.5–5.0	1.0–5.0
Total data	974	936	1667
Total unique data	398	559	935
Observed data, ($I > 3\sigma(I)$)	381	427	708
Data collected	−3,15 −3,11 −1,3	−1,16 −1,12 −1,4	−13,13 −1,16 −1,4
Merging R	1.87	5.00	7.12
Abs. correction range	1.34–1.97	1.00–1.85	1.00–1.51
No. of refined parameters	62	61	77
Weights (*16*)	10.24, 0.41, 7.49	2.48, 1.87, 1.83	2.11, 0.75, 1.45
Extinction parameter	8.8(8)	—	18(2)
Final shift/error	0.004	0.0005	0.0035
Max. residual electron density (e Å^{-3})	0.64	2.2	2.0
Final R, R_w	4.07, 4.49	4.44, 4.85	4.59, 5.83

restraints to the total Co : Al ratio were applied. After application of a polynomial weighting scheme (which downweighted the 16,0,0 reflection) the refinement converged to a final R-factor of 4.44% (Table I). An extinction correction was not needed. Fractional atomic coordinates, occupation numbers, and anisotropic temperature factors are listed in Table III, and selected distances and angles are presented in Table VI.

For Cu_2AlBO_5 the systematic absences were consistent with the space group $P2_1/a$. The structure was solved by Patterson and difference Fourier techniques. The empirical absorption program DIFABS (*21*) was used, as initial attempts to refine the anisotropic temperature factors led to nonpositive definite ellipses. Final refinement of the fractional atomic coordinates, anisotropic temperature factors, constrained metal site occupancies (as per the nickel compound), and an extinction parameter converged to give an R-value of 4.55%. The results are summarized in Table I, with final fractional atomic coordinates, occupation numbers, and anisotropic temperature factors presented in Table IV. Selected distances and angles listed in Table VII.

Madelung calculations were performed

TABLE II

ATOMIC PARAMETERS FOR Ni_2AlBO_5[a]

Atom	x/a	y/b	z/c	Fractional occ.
Ni(1)	0.28050(6)	−0.00198(7)	0.50000	0.890(4)
Al(1)	0.28050(6)	−0.00198(7)	0.50000	0.110(4)
Ni(2)	0.00000	0.00000	0.50000	0.852(4)
Al(2)	0.00000	0.00000	0.50000	0.148(4)
Ni(3)	0.00000	0.50000	0.00000	0.652(4)
Al(3)	0.00000	0.50000	0.00000	0.348(4)
Ni(4)	0.11430(8)	0.2373(1)	0.00000	0.358(4)
Al(4)	0.11430(8)	0.2373(1)	0.00000	0.642(4)
B(1)	0.3610(4)	0.2727(6)	0.00000	
O(1)	0.4591(2)	0.3485(3)	0.00000	
O(2)	0.1433(2)	0.1102(4)	0.50000	
O(3)	0.3610(2)	0.1204(4)	0.00000	
O(4)	0.0748(3)	0.3829(3)	0.50000	
O(5)	0.2602(2)	0.3444(3)	0.00000	

Atom	U_{11}	U_{22}	U_{33}	U_{23}	U_{13}	U_{12}
M(1)	0.0063(5)	0.0085(6)	0.0078(6)	0	0	0.0004(2)
M(2)	0.0061(7)	0.0068(7)	0.0077(8)	0	0	−0.0002(3)
M(3)	0.0071(7)	0.0106(8)	0.0075(8)	0	0	−0.0003(4)
M(4)	0.0073(6)	0.0074(6)	0.0069(6)	0	0	−0.0007(4)
B(1)	0.0094(23)	0.0088(24)	0.0070(24)	0	0	−0.0009(15)
O(1)	0.0084(14)	0.0126(15)	0.0118(15)	0	0	−0.0012(12)
O(2)	0.0090(16)	0.0091(17)	0.0166(19)	0	0	0.0006(10)
O(3)	0.0102(16)	0.0097(17)	0.0117(17)	0	0	−0.0001(10)
O(4)	0.0096(14)	0.0098(14)	0.0335(20)	0	0	0.0000(11)
O(5)	0.0087(13)	0.0100(14)	0.0116(13)	0	0	−0.0001(12)

[a] Anisotropic temperature factors are of the form $\exp[-2\pi^2(U_{11}h^2a^{*2} + \cdots + 2U_{12}hka^*b^* + \cdots)]$.

using MADELUNG, a locally written computer program which uses the method of van Gool and Picken (*22*).

Results and Discussion

We have established a program to synthesize new ternary transition metal borates and examine their properties. Flux methods were explored to facilitate the isolation of single crystals. Borax was chosen, as it is known to be an excellent medium for the growth of crystals and would also give a ready supply of both sodium and borate ions. Analytical electron microscopy results indicated that the initial reactions with NiO or CuO led to the synthesis of aluminoborates, with the alumina boat acting as the source of aluminium cations. The reaction with Co_3O_4 was performed with added aluminium oxide, and qualitatively appeared to give an increased yield of product. We did not observe any evidence for sodium incorporation into any of the crystalline products.

Analytical electron microscopy was performed for all of the compounds. For Ni_2AlBO_5, the analysis of several crystallites led to a calculated Ni:Al ratio of 2.2(2):1. For $Co_{2.1}Al_{0.9}BO_5$ the value was 2.8(3):0.9 and for Cu_2AlBO_5 it was 2.3(2):1. The values all agree reasonably well with the true stoichiometries, but are consistently high and have rather large estimated standard deviations. A possible reason for this is the fluorescence of the aluminium K_α line by the metal K_β lines.

The nickel and cobalt compounds crystallize with the ludwigite structure (Fig. 1) in which there are four crystallographically

TABLE III

ATOMIC PARAMETERS FOR $Co_{2.1}Al_{0.9}BO_5$[a]

Atom	x/a	y/b	z/c	Fractional occ.
Co(1)	0.27811(7)	−0.00239(7)	0.50000	0.850(14)
Al(1)	0.27811(7)	−0.00239(7)	0.50000	0.150(14)
Co(2)	0.00000	0.00000	0.50000	0.788(10)
Al(2)	0.00000	0.00000	0.50000	0.212(10)
Co(3)	0.00000	0.50000	0.00000	0.592(10)
Al(3)	0.00000	0.50000	0.00000	0.408(10)
Co(4)	0.11365(7)	0.23879(9)	0.00000	0.544(13)
Al(4)	0.11365(7)	0.23879(9)	0.00000	0.456(13)
B(1)	0.3609(4)	0.2699(7)	0.00000	
O(1)	0.4594(3)	0.3468(4)	0.00000	
O(2)	0.1246(3)	0.1108(4)	0.50000	
O(3)	0.3632(3)	0.1210(4)	0.00000	
O(4)	0.0744(4)	0.3857(4)	0.50000	
O(5)	0.2605(3)	0.3405(4)	0.00000	

Atom	U_{11}	U_{22}	U_{33}	U_{23}	U_{13}	U_{12}
M(1)	0.0108(5)	0.0020(4)	0.0051(4)	0	0	0.0008(2)
M(2)	0.0107(7)	0.0005(6)	0.0048(6)	0	0	−0.0008(3)
M(3)	0.0090(7)	0.0025(7)	0.0050(7)	0	0	0.0000(3)
M(4)	0.0113(5)	0.0015(5)	0.0045(5)	0	0	−0.0016(3)
B(1)	0.0137(26)	0.0102(29)	0.0017(22)	0	0	−0.0019(17)
O(1)	0.0189(20)	0.0113(20)	0.0115(19)	0	0	−0.0033(14)
O(2)	0.0093(18)	0.0130(22)	0.0205(22)	0	0	−0.0002(11)
O(3)	0.0168(20)	0.0069(19)	0.0146(20)	0	0	0.0010(10)
O(4)	0.0202(19)	0.0013(19)	0.0467(27)	0	0	−0.0009(12)
O(5)	0.0178(18)	0.0111(18)	0.0113(19)	0	0	0.0040(13)

[a] Anisotropic temperature factors are of the form $\exp[-2\pi^2(U_{11}h^2a^{*2} + \cdots + 2U_{12}hka^*b^* + \cdots)]$.

TABLE IV

ATOMIC PARAMETERS FOR Cu_2AlBO_5[a]

Atom	x/a	y/b	z/c	Fractional occ.
Cu(1)	−0.00718(9)	0.28012(7)	0.0403(3)	0.960(6)
Al(1)	−0.00718(9)	0.28012(7)	0.0403(3)	0.040(6)
Cu(2)	0.00000	0.00000	0.00000	0.925(8)
Al(2)	0.00000	0.00000	0.00000	0.075(8)
Cu(3)	0.00000	0.50000	0.50000	0.411(8)
Al(3)	0.00000	0.50000	0.50000	0.589(8)
Cu(4)	−0.2307(1)	−0.1165(1)	−0.5714(4)	0.372(7)
Al(4)	−0.2307(1)	−0.1165(1)	−0.5714(4)	0.628(7)
B(1)	0.2347(8)	−0.1359(6)	0.4649(26)	
O(1)	0.1055(6)	0.1438(4)	0.0408(19)	
O(2)	0.1573(5)	−0.0383(4)	0.4829(15)	
O(3)	0.1167(5)	0.3671(4)	0.5048(16)	
O(4)	−0.1134(8)	0.4252(6)	0.0020(35)	
O(5)	−0.1689(5)	0.2394(4)	−0.4135(16)	

Atom	U_{11}	U_{22}	U_{33}	U_{23}	U_{13}	U_{12}
M(1)	0.0074(4)	0.0070(5)	0.0086(4)	−0.0010(3)	0.0002(3)	0.0006(3)
M(2)	0.0054(6)	0.0074(6)	0.0060(6)	0.0001(4)	0.0013(4)	−0.0018(4)
M(3)	0.0068(9)	0.0079(9)	0.0069(9)	−0.0011(5)	0.0029(6)	0.0000(5)
M(4)	0.0064(6)	0.0067(6)	0.0068(7)	0.0009(4)	0.0009(4)	−0.0011(4)
B(1)	0.0057(29)	0.0063(28)	0.0122(31)	−0.0002(22)	0.0011(24)	0.0017(23)
O(1)	0.0180(25)	0.0094(22)	0.0195(26)	0.0006(18)	−0.0063(21)	−0.0048(18)
O(2)	0.0124(21)	0.0072(20)	0.0107(20)	0.0019(16)	0.0024(17)	0.0023(17)
O(3)	0.0098(21)	0.0124(21)	0.0105(22)	0.0004(16)	0.0007(17)	−0.0013(16)
O(4)	0.0329(40)	0.0140(29)	0.1111(77)	−0.0304(37)	−0.0526(48)	0.0151(28)
O(5)	0.0108(21)	0.0073(20)	0.0139(24)	−0.0033(16)	0.0008(17)	−0.0030(17)

[a] Anisotropic temperature factors are of the form $\exp[-2\pi^2(U_{11}h^2a^{*2} + \cdots + 2U_{12}hka^*b^* + \cdots)]$.

distinct metal sites. Each of these positions contains a mixture of transition metal and aluminium ions in slightly distorted octahedral coordination (Tables V and VI). All of the atoms have integral or half-integral *z*-coordinates. This leads to a lamellar network of metal–oxygen octahedra that can be easily visualized by considering two different *ab*-planes. The metal–oxygen polyhedra centered at $z = 0$ exist as units of three edge-sharing octahedra linked by trigonal BO_3 groups to form an infinite two-dimensional network (Fig. 2). The second layer, centered at $z = \frac{1}{2}$, is composed of discrete groups of three corner-sharing metal–oxygen octahedra (Fig. 3). These two slabs are joined together by the sharing of oxygen atoms to give the three-dimensional structure, with the octahedra between these two planes sharing both corners and edges.

The structure of Cu_2AlBO_5 is related to the other two by a monoclinic distortion of approximately 8°. This is most easily seen by comparing a view of the structures of the nickel and copper compounds (Fig. 4). An examination of the metal coordination environments (Table VII) in this structure reveals large deviations from octahedral symmetry. These are responsible for lowering

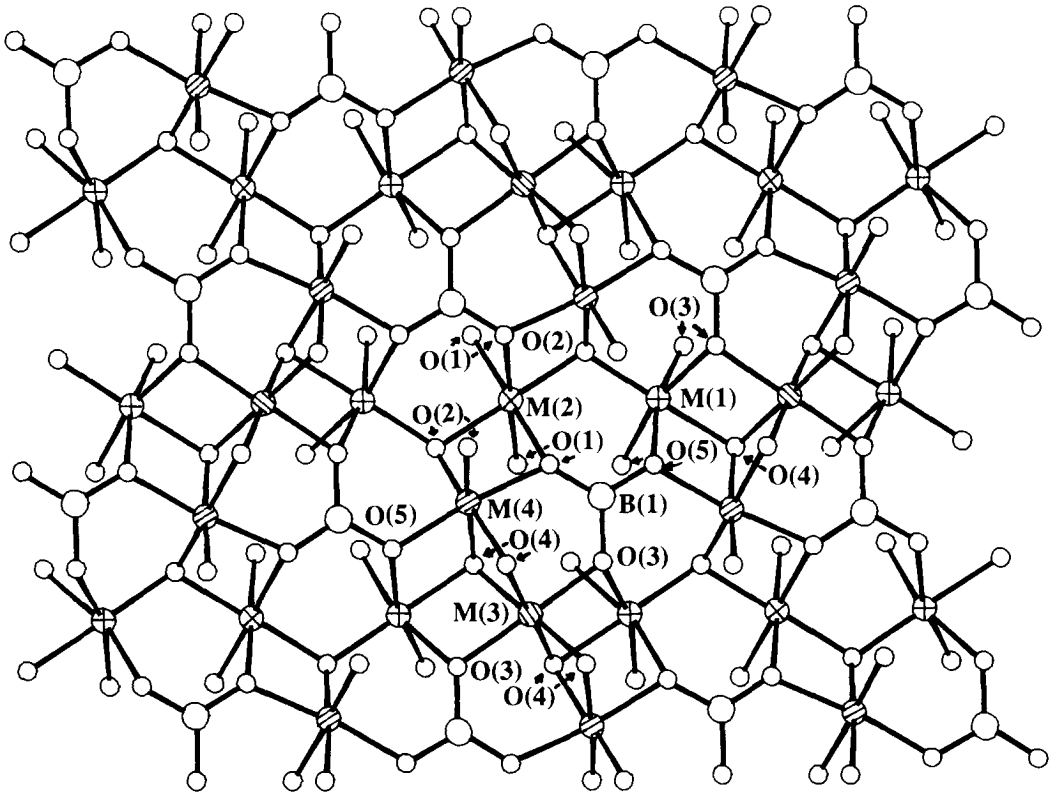

FIG. 1. A view of the structure of Ni_2AlBO_5 approximately along the *c*-axis, showing the atomic labeling.

the symmetry of the Bravais lattice, and can be explained by a Jahn–Teller distortion caused by the presence of copper(II). For sites 1 and 2, the coordination is best described as [4 + 2], with the axial *M*–O bonds approximately 20% longer than the equatorial bonds. Sites 3 and 4 have more regular coordination, although for *M*(4) the coordination appears to be nearly square pyramidal, with a sixth oxygen atom approximately 0.5 Å further away. This oxygen atom, O(4), has an anomalously high temperature factor, possibly indicating disorder over two sites. Attempts to model this situation, however, failed.

There are four metal sites in each of these structures, and all of them contain different amounts of transition metal and aluminum atoms (Tables II–IV). The occupations consistently fall into two groups. The first two sites in each compound have the greatest amount of divalent metal, 79–96%, while positions 3 and 4 have significantly less. For the nickel and cobalt phases, the effect of this change in M^{2+} : Al^{3+} ratio is a reduction of the site atomic radii with decreasing divalent metal content. This leads to a linear reduction of the average *M*–O bond length (Tables V and VI) with aluminium content. For the copper compound, the situation is complicated by the observed Jahn–Teller distortions. However, it is clear that sites 1 and 2 have a typical copper(II) environment, i.e., [4 + 2], while sites 3 and 4 are midway between [4 + 2] and octahedral coordination.

Thus all three compounds display an interesting disorder of divalent and trivalent

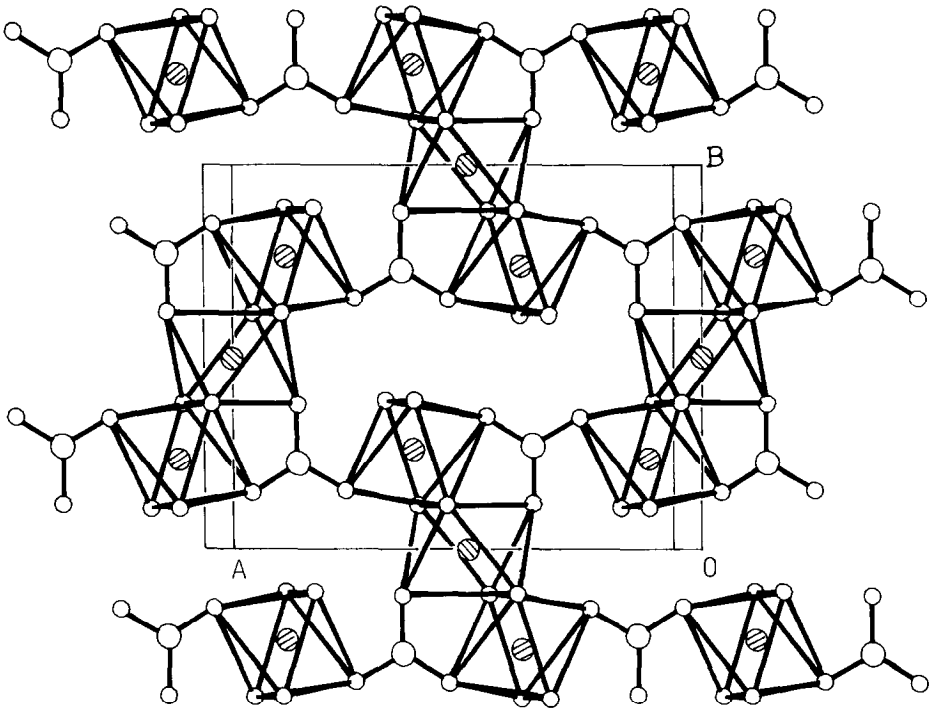

FIG. 2. A view of the polyhedra centered at $z = 0$ for Ni_2AlBO_5.

atoms over the four metal sites. A common feature is the preferential occupation of positions 1 and 2 by the divalent metal atoms. A qualitative picture of why this occurs can be drawn by a closer inspection of the oxygen atoms. Metal sites 1 and 2 sit in the

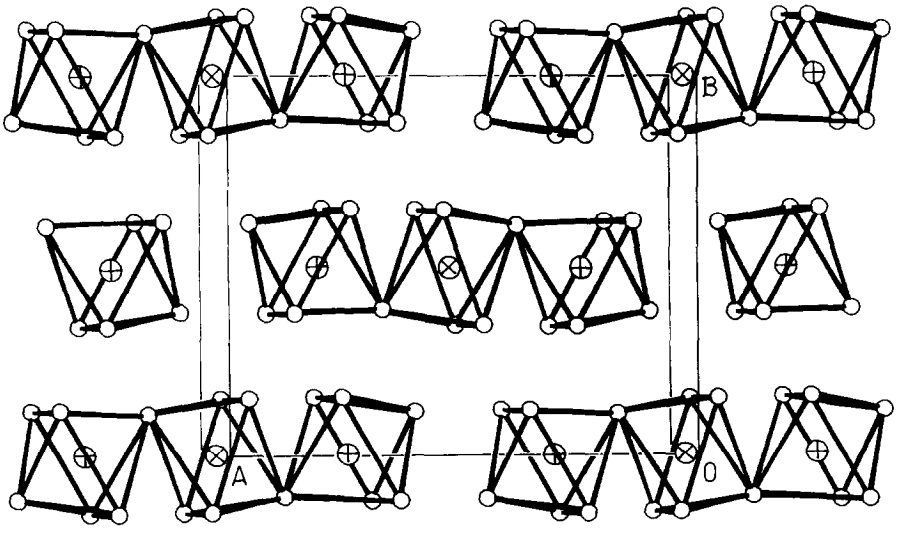

FIG. 3. A view of the polyhedra centered at $z = \frac{1}{2}$ for Ni_2AlBO_5.

TABLE V

SELECTED DISTANCES (Å) AND ANGLES (°) FOR Ni_2AlBO_5

M(1)–O(2)	1.939(3)	O(3)–*M*(1)–O(2)	2 × 96.5(1)
M(1)–O(3)	2 × 2.084(2)	O(3)–*M*(1)–O(3)	89.8(1)
M(1)–O(4)	2.030(3)	O(4)–*M*(1)–O(2)	179.3(1)
M(1)–O(5)	2 × 2.089(2)	O(4)–*M*(1)–O(3)	2 × 83.0(1)
		O(5)–*M*(1)–O(2)	2 × 98.9(1)
average = 2.052		O(5)–*M*(1)–O(3)	2 × 88.27(9)
		O(5)–*M*(1)–O(3)	2 × 164.7(1)
		O(5)–*M*(1)–O(4)	2 × 81.6(1)
		O(5)–*M*(1)–O(5)	89.6(1)
M(2)–O(1)	4 × 2.076(2)	O(1)–*M*(2)–O(1)	2 × 90.2(1)
M(2)–O(2)	2 × 1.993(3)	O(1)–*M*(2)–O(1)	2 × 89.8(1)
		O(1)–*M*(2)–O(1)	2 × 180.00
average = 2.048		O(2)–*M*(2)–O(1)	4 × 97.5(1)
		O(2)–*M*(2)–O(1)	4 × 82.5(1)
		O(2)–*M*(2)–O(2)	180.00
M(3)–O(3)	2 × 1.997(3)	O(3)–*M*(3)–O(3)	180.00
M(3)–O(4)	4 × 2.027(2)	O(4)–*M*(3)–O(3)	4 × 85.3(1)
		O(4)–*M*(3)–O(3)	4 × 94.7(1)
average = 2.017		O(4)–*M*(3)–O(4)	2 × 93.1(1)
		O(4)–*M*(3)–O(4)	2 × 86.9(1)
		O(4)–*M*(3)–O(4)	2 × 180.00
M(4)–O(1)	2.021(3)	O(2)–*M*(4)–O(1)	2 × 86.2(1)
M(4)–O(2)	2 × 1.905(2)	O(2)–*M*(4)–O(2)	101.1(2)
M(4)–O(4)	2 × 2.037(2)	O(4)–*M*(4)–O(1)	2 × 92.1(1)
M(4)–O(5)	2.006(3)	O(4)–*M*(4)–O(2)	2 × 83.2(1)
		O(4)–*M*(4)–O(2)	2 × 175.3(1)
average = 1.985		O(5)–*M*(4)–O(1)	173.7(1)
		O(5)–*M*(4)–O(2)	2 × 97.8(1)
		O(4)–*M*(4)–O(4)	92.5(1)
		O(5)–*M*(4)–O(4)	2 × 83.5(1)
B(1)–O(1)	1.366(5)	O(3)–B(1)–O(1)	120.4(4)
B(1)–O(3)	1.388(6)	O(5)–B(1)–O(1)	121.3(5)
B(1)–O(5)	1.376(6)	O(5)–B(1)–O(3)	118.3(4)

nonborate layer and have four of six oxygen atoms from borate groups above and below this plane. For sites 3 and 4, only two of the four oxygen atoms are from borate groups. If one considers the covalency of B–O bonds, then each borate oxygen atom can be considered closer to O^- than to O^{2-}. Thus one would anticipate placing the divalent cation on the sites of lower charge, i.e., sites 1 and 2.

Another important aspect that affects the site potentials is the connectivity of the octahedra. In complicated structures, these effects are most easily estimated by performing Madelung calculations. Assuming a random charge distribution of +2.33 on each site, to avoid biasing the results, the calculations clearly show that sites 1 and 2 have less negative potentials than 3 and 4 (Table VIII). We would thus expect them to contain more of the divalent cations, again corroborating the experimental observations.

This pattern of partial ordering contrasts sharply with the results for ludwigite (*5*), where three sites are reported to contain only magnesium(II) ions and one site iron(III) ions. Our results for Ni_2AlBO_5 also contradict an earlier report (*7*) where random distribution of the metals was assumed. As the fractional atomic coordinates for these two determinations are

TABLE VI

SELECTED DISTANCES (Å) AND ANGLES (°) FOR $Co_{2.1}Al_{0.9}BO_5$

M(1)–O(2)	1.932(4)	O(3)–*M*(1)–O(2)	2 × 96.7(1)
M(1)–O(3)	2 × 2.139(3)	O(3)–*M*(1)–O(3)	88.8(1)
M(1)–O(4)	2.049(4)	O(4)–*M*(1)–O(2)	177.6(2)
M(1)–O(5)	2 × 2.131(3)	O(4)–*M*(1)–O(3)	2 × 81.6(1)
		O(5)–*M*(1)–O(2)	2 × 100.5(1)
average = 2.087		O(5)–*M*(1)–O(3)	2 × 88.4(1)
		O(5)–*M*(1)–O(3)	2 × 162.8(2)
		O(5)–*M*(1)–O(4)	2 × 81.2(1)
		O(5)–*M*(1)–O(5)	89.2(1)
M(2)–O(1)	4 × 2.113(3)	O(1)–*M*(2)–O(1)	2 × 90.2(1)
M(2)–O(2)	2 × 1.993(3)	O(1)–*M*(2)–O(1)	2 × 89.8(1)
		O(1)–*M*(2)–O(1)	2 × 180.0
average = 2.073		O(2)–*M*(2)–O(1)	4 × 98.2(1)
		O(2)–*M*(2)–O(1)	4 × 81.8(1)
		O(2)–*M*(2)–O(2)	180.00
M(3)–O(3)	2 × 1.984(3)	O(3)–*M*(3)–O(3)	180.00
M(3)–O(4)	4 × 2.036(3)	O(4)–*M*(3)–O(3)	4 × 85.8(1)
		O(4)–*M*(3)–O(3)	4 × 94.2(1)
average = 2.019		O(4)–*M*(3)–O(4)	2 × 94.6(2)
		O(4)–*M*(3)–O(4)	2 × 85.4(2)
		O(4)–*M*(3)–O(4)	2 × 180.00
M(4)–O(1)	2.013(4)	O(2)–*M*(4)–O(1)	2 × 85.9(1)
M(4)–O(2)	2 × 1.936(3)	O(2)–*M*(4)–O(2)	101.3(2)
M(4)–O(4)	2 × 2.070(3)	O(4)–*M*(4)–O(1)	2 × 92.6(1)
M(4)–O(5)	1.997(4)	O(4)–*M*(4)–O(2)	2 × 83.0(1)
		O(4)–*M*(4)–O(2)	2 × 175.3(1)
average = 2.004		O(5)–*M*(4)–O(1)	175.1(1)
		O(5)–*M*(4)–O(2)	2 × 97.2(1)
		O(4)–*M*(4)–O(4)	92.6(1)
		O(5)–*M*(4)–O(4)	2 × 84.0(1)
B(1)–O(1)	1.378(6)	O(3)–B(1)–O(1)	119.7(5)
B(1)–O(3)	1.370(7)	O(5)–B(1)–O(1)	120.8(5)
B(1)–O(5)	1.369(7)	O(5)–B(1)–O(3)	119.5(4)

TABLE VII

SELECTED DISTANCES (Å) AND ANGLES (°) FOR Cu_2AlBO_5

$M(1)$–O(1)	1.921(5)	O(3)–$M(1)$–O(1)	92.4(2)	O(3)–$M(1)$–O(1)	99.3(2)
$M(1)$–O(3)	2.370(5)	O(3)–$M(1)$–O(3)	89.0(2)	O(4)–$M(1)$–O(1)	175.1(4)
$M(1)$–O(3)	1.997(5)	O(4)–$M(1)$–O(3)	82.7(4)	O(4)–$M(1)$–O(3)	80.7(2)
$M(1)$–O(4)	1.973(6)	O(5)–$M(1)$–O(1)	99.6(2)	O(5)–$M(1)$–O(3)	90.9(2)
$M(1)$–O(5)	1.975(5)	O(5)–$M(1)$–O(3)	161.1(2)	O(5)–$M(1)$–O(4)	80.5(2)
$M(1)$–O(5)	2.453(5)	O(5)–$M(1)$–O(1)	103.0(2)	O(5)–$M(1)$–O(3)	164.6(2)
		O(5)–$M(1)$–O(3)	87.9(2)	O(5)–$M(1)$–O(4)	81.8(4)
		O(5)–$M(1)$–O(5)	87.2(2)		
$M(2)$–O(1)	2 × 1.956(5)	O(1)–$M(2)$–O(1)	180.00	O(2)–$M(2)$–O(1)	2 × 81.5(2)
$M(2)$–O(2)	2 × 1.997(5)	O(2)–$M(2)$–O(1)	2 × 98.5(2)	O(2)–$M(2)$–O(1)	2 × 80.3(2)
$M(2)$–O(2)	2 × 2.350(5)	O(2)–$M(2)$–O(1)	2 × 99.7(2)	O(2)–$M(2)$–O(2)	2 × 89.5(2)
		O(2)–$M(2)$–O(2)	2 × 90.5(2)	O(2)–$M(2)$–O(2)	2 × 180.00
$M(3)$–O(3)	2 × 1.908(5)	O(3)–$M(3)$–O(3)	180.00	O(4)–$M(3)$–O(3)	2 × 83.5(2)
$M(3)$–O(4)	2 × 1.951(7)	O(4)–$M(3)$–O(3)	2 × 96.5(2)	O(4)–$M(3)$–O(3)	2 × 89.8(2)
$M(3)$–O(4)	2 × 2.17(1)	O(4)–$M(3)$–O(3)	2 × 90.2(2)	O(4)–$M(3)$–O(4)	2 × 96.2(3)
		O(4)–$M(3)$–O(4)	2 × 83.8(2)	O(4)–$M(3)$–O(4)	2 × 180.00
$M(4)$–O(1)	2.003(6)	O(1)–$M(4)$–O(1)	103.7(3)	O(2)–$M(4)$–O(1)	91.2(2)
$M(4)$–O(2)	1.903(5)	O(2)–$M(4)$–O(1)	92.7(2)	O(4)–$M(4)$–O(1)	90.5(4)
$M(4)$–O(4)	1.955(5)	O(4)–$M(4)$–O(1)	165.5(4)	O(4)–$M(4)$–O(2)	94.5(2)
$M(4)$–O(5)	1.899(6)	O(4)–$M(4)$–O(1)	177.7(2)	O(4)–$M(4)$–O(1)	77.4(2)
$M(4)$–O(4)	2.47(1)	O(4)–$M(4)$–O(2)	86.9(2)	O(4)–$M(4)$–O(4)	88.3(3)
$M(4)$–O(5)	1.937(5)	O(5)–$M(4)$–O(1)	99.9(2)	O(5)–$M(4)$–O(1)	96.6(2)
		O(5)–$M(4)$–O(2)	168.7(2)	O(5)–$M(4)$–O(4)	83.4(2)
		O(5)–$M(4)$–O(4)	82.0(2)		
B(1)–O(2)	1.364(8)	O(3)–B(1)–O(2)	120.7(6)		
B(1)–O(3)	1.382(8)	O(5)–B(1)–O(2)	121.5(6)		
B(1)–O(5)	1.366(8)	O(5)–B(1)–O(3)	117.8(6)		

TABLE VIII

MADELUNG RESULTS

Site	Nominal charge	Calculated site potential	% Al (experimental)
		Ni_2AlBO_5	
$M(1)$	2.33	−2.18	11.0
$M(2)$	2.33	−2.17	14.8
$M(3)$	2.33	−2.29	34.8
$M(4)$	2.33	−2.37	64.2
		$Co_{2.1}Al_{0.9}BO_5$	
$M(1)$	2.33	−2.18	15
$M(2)$	2.33	−2.17	21
$M(3)$	2.33	−2.29	41
$M(4)$	2.33	−2.37	46
		Cu_2AlBO_5	
$M(1)$	2.33	−2.04	4.0
$M(2)$	2.33	−1.99	7.5
$M(3)$	2.33	−2.27	58.9
$M(4)$	2.33	−2.23	62.8

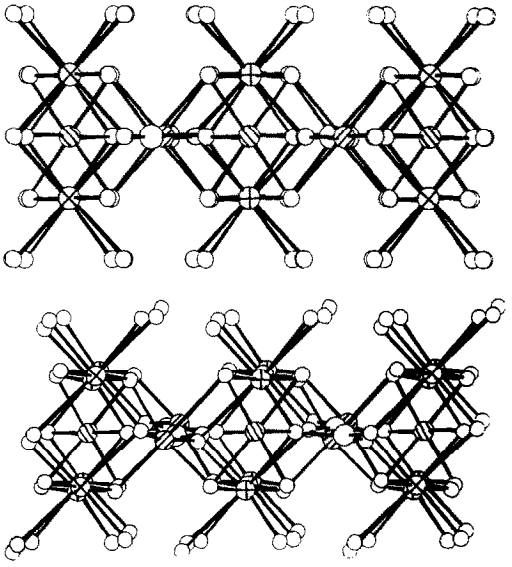

FIG. 4. Comparative views of Ni_2AlBO_5 (top) and Cu_2AlBO_5 (bottom).

similar, our significantly lower agreement factor, 4 vs 17%, indicates our model is much more accurate. It is also interesting to note that reports for the related materials $Ni_5MB_2O_{10}$ (M = Ti (*8, 10*), Zr, and Ge (*11*)) show that these compounds exhibit metal disorder on only one site.

Although both covalent and ionic considerations point to the observed pattern of metal site preference, neither method quantitatively predicts the experimental results nor the observed differences from compound to compound. Further work is in progress to better understand the site preference of metals in these and other mixed-metal borate systems.

Acknowledgments

The authors thank Dr. D. J. Watkin for helpful advice on the crystallographic work. J.A.H. thanks the SERC and Amoco Chemical Co. for financial support. L.C.S. thanks P. K. Mayo and G. A. Velligan for their technical support and J. A. Kaduk for crystallographic support.

References

1. L. C. Satek, U.S. Patent 4,590,324 (1986).
2. G. P. Hussman and P. E. McMahon, U.S. Patent 4,740,647 (1988).
3. A. A. Ballman, *Amer. Mineral.* **47,** 1380 (1962).
4. D. Eimerl, L. Davis, S. Velsko, E. K. Graham, and A. Zalkin, *J. Appl. Phys.* **62,** 1968 (1987).
5. Y. Takeuchi, T. Watanabe, and T. Ito, *Acta Crystallogr.* **3,** 98 (1950).
6. E. F. Bertaut, *Acta Crystallogr.* **3,** 473 (1950).
7. A. M. Schwab and E. F. Bertaut, *Bull. Soc. Fr. Mineral. Cristallogr.* **93,** 255 (1970).
8. C. G. F. Stenger, G. C. Verschoor, and D. J. W. Ijdo, *Mater. Res. Bull.* **8,** 1285 (1973).
9. L. Richter, Ph.D. thesis, Aachen University, FDR (1977).
10. Th. Armbruster and G. A. Lager, *Acta Crystallogr.* **C41,** 1400 (1985).
11. K. Bluhm and H. K. Muller-Buschbaum, *J. Less-Common Met.* **147,** 133 (1989).
12. Uhlig *et al.*, JCPDS Grant-in-Aid Report (1976).
13. L. C. Satek, J. A. Hriljac, R. D. Brown, J. A. Kaduk, and A. K. Cheetham, in preparation.
14. A. K. Cheetham and A. J. Skarnulis, *Anal. Chem.* **53,** 1060 (1981).
15. A. C. T. North, D. C. Phillips, and F. S. Mathews, *Acta Crystallogr.* **A24,** 351 (1968).
16. E. Prince, "Mathematical Techniques in Crystallography," Springer-Verlag, New York (1982).
17. P. D. Baird, "RC85: User's Guide," Chemical Crystallography Lab, Oxford University, Oxford, UK (1987).
18. D. J. Watkin, J. R. Carruthers, and P. W. Betteridge, "CRYSTALS-User's Guide," Chemical Crystallography Lab, Oxford University, Oxford, UK (1985).
19. "International Tables for X-Ray Crystallography," Vol. IV, Kynoch Press, Birmingham, UK (1974).
20. Developed and distributed by Chemical Design, Ltd., Oxford, UK.
21. N. Walker and D. Stuart, *Acta Crystallogr.* **A39,** 158 (1983).
22. W. van Gool and A. G. Piken, *J. Mater. Sci.* **4,** 95 (1969).